Finite-size studies of phases and dimerization in one-dimensional extended Peierls-Hubbard models

V. Waas, H. Büttner, and J. Voit*
Physikalisches Institut, Universität Bayreuth, 8580 Bayreuth, West Germany
(Received 2 June 1989; revised manuscript received 6 November 1989)

We study extended Hubbard and Peierls-Hubbard models with up to $N=10$ sites and half-filled bands with modified boundary conditions. For the extended Hubbard model, the finite-size dependence of the transition from the charge-density-wave regime (CDW) to the spin-density-wave (SDW) regime and of the condensation transition is critically examined, clarifying some previous results. For the Peierls-Hubbard model and $N \leq 10$ with modified periodic boundary conditions, we always see a decrease of dimerization with U. Extrapolating these results to infinite N, we find that dimerization is enhanced by U for small electron-phonon coupling $\tilde{\alpha} < 0.75$, whereas it decreases with U for $0.75 < \tilde{\alpha} \leq 1$. By extending this model by a nearest-neighbor repulsion V, the amplitude of dimerization reaches a maximum at the same value $U \leq 2V$, where the CDW-to-SDW transition occurs in the extended Hubbard model.

I. INTRODUCTION

Recently there has been a renewed interest in the Hubbard model[1] and various extensions and geometries in one and two dimensions. Whereas the two-dimensional (2D) Hubbard model plays an important role in the discussion on the high-T_c superconductors,[2] the one-dimensional (1D) Hubbard model is either the very basis of or a relevant extension to theories describing quasi-one-dimensional compounds such as conducting polymers and organic superconductors.[3] The standard model for the description of conducting polymers was proposed by Su, Schrieffer, and Heeger[4] (SSH). It considers the bond alternation in conjugated polymers to be the result of a Peierls distortion, and consequently starts out from a tight-binding Hamiltonian of noninteracting electrons on an elastic lattice. While the SSH model describes a variety of experimental results quite well, some others are in qualitative disagreement and point towards the necessity to include (possibly strong) electron-electron interactions. For example, there are observations of negative spin densities on odd sites of neutral solitons in electron-nuclear-double-resonance experiments,[5,6] and the finding that neutral solitons do not contribute to the midgap optical absorption.[7] When the SSH model is extended by adding Coulomb interactions between the electrons, one is faced with a complicated many-body problem, namely, the competition of the attractive electron-phonon with the repulsive electron-electron interactions, both being associated with very different energy scales. In polyacetylene, e.g., the electronic bandwidth is believed to be about 10 eV, while a characteristic phonon frequency is estimated[4] as 0.1 eV. Accordingly, initial results on the influence of a Hubbard on-site electron repulsion U on dimerization—certainly the most fundamental property of conjugated polymers—were very surprising: As U is increased from zero, the dimerization first increases, then passes through a maximum and finally decreases.[8–14] Although there seems to be a common agreement about the qualitative features of this behavior, we shall show that it may no longer be true if the electron-lattice coupling is strong. Even for weaker coupling important unsolved questions remain. For example, both the location of the dimerization maximum as a function of U and the amount of dimerization enhancement are different in different studies. Worse, even the mechanisms operating are disputed: Some authors find the dimerization maximum to occur for U close to the bandwidth $4t_0$ of the noninteracting undimerized (i.e., metallic) system and to be determined by a barrier of resonance between different configurations of valence bonds, i.e., different symmetry-broken real-space configurations;[11] others argue about the relative importance of the Peierls and Hubbard gaps;[9] finally, a very recent study obtains the dimerization maximum as a result of a competition between the dimerization gap at $U=0$ and the actual valence-band width[14] (i.e., finite U, finite dimerization). This situation is certainly due to different approximations used in the various approaches. Analytic calculations often rely on perturbation expansions and therefore small parameters,[9,10,12,13] while the small system size, implying an extreme sensitivity of the results to boundary conditions, is the most serious limitation of the "in principle exact" numerical methods.[8,11] In Ref. 14 a systematic finite-size analysis of numerical data on SSH-Hubbard and Pariser-Parr-Pople (PPP) models were performed, shedding, however, additional doubt on the reliability of previous results.[8–13] Therefore more systematic studies are certainly helpful in clarifying these issues. This applies in particular to extensions of the electron-electron Hamiltonian beyond the simple Hubbard model, where only few studies are available[8,11] and even the purely electronic Hamiltonian is not fully understood.[15–18]

This paper attempts to clarify some of these issues by performing Lanczos diagonalization studies of extended Hubbard and Peierls-Hubbard models with half-filled

bands. After the definition of the model and a general discussion of boundary conditions in Sec. II, we investigate the 1D extended Hubbard model, which consists of a nearest-neighbor hopping element (t_0) and electronic on-site (U) and intersite (V) interactions, in Sec. III. This model shows a phase transition from a charge-density-wave (CDW) region (with alternating doubly occupied and empty sites) to a spin-density-wave (SDW) ground state (with antiferromagentically ordered spins) for repulsive interactions. Based on the exact computation of eigenstates and correlation functions, we examine the nature of the transition and its location in the U-V plane, which have been controversial questions so far.[15–18] We also investigate the condensation transition for attractive interactions,[19] where we present results on an intermediate region between the charge separated (CS) and the SDW phase.

In Sec. IV, the electrons are coupled to acoustic phonons in an elastic (but static) lattice, as proposed by Su, Schrieffer, and Heeger.[4] We examine the influence of a Hubbard U on dimerization for various strengths of the electron-phonon coupling. It will be seen that the parameters believed to describe polyacetylene[4] are intermediate between small and strong coupling and that important new physics emerges in these limits. Finally, we add a nearest-neighbor interaction V. We shall point out that the magnitude of dimerization in these (finite) systems is intimately related to the CDW-to-SDW transition of the extended Hubbard model, and discuss its consequences.

We find that often finite-size effects have been underestimated earlier and are indeed responsible for much of the confusion in the literature. On selected examples, we demonstrate that a careful finite-size analysis is essential for obtaining *reliable* information on infinite systems. A conclusing summary can be found in Sec. V.

II. MODEL AND BOUNDARY CONDITIONS

We consider the following SSH-Hubbard Hamiltonian

$$H=-\sum_{l,s}[t_0+\alpha(-1)^l X](c^{\dagger}_{l+1,s}c_{l,s}+\text{H.c.}) + U\sum_l n_{l\uparrow}n_{l\downarrow}+V\sum_l n_l n_{l+1}+NKX^2/2\ . \tag{1}$$

As we are interested in the half-filled band case, there are N electrons with spin s described by creation operators $c^{\dagger}_{l,s}$ distributed on the N lattice sites labeled with $l=1,2,\ldots,N$. $n_{l,s}=c^{\dagger}_{l,s}c_{l,s}$ is the number operator of electrons with spin s on site l, and $n_l=n_{l\uparrow}+n_{l\downarrow}$. $t_l=t_0+\alpha(-1)^l X$ is the transfer element for nearest-neighbor hopping between l and $l+1$, which is modulated by a static dimerization of amplitude X; thus, $(-1)^l X$ is the difference between the distortions at L and $l+1$. α is the electron-phonon coupling[4] and K the force constant of the lattice. The electrons interact through an on-site repulsion U and a nearest-neighbor interaction V.

A crucial point is the selection of appropriate and consistent boundary conditions, as the solutions of the Hamiltonian (1) quantitatively depend on the number of sites (and of electrons) N, and even qualitatively on the boundary conditions chosen. This will be easily seen in the noninteracting limit $U=V=0$, where the Hamiltonian (1) can be solved analytically by filling $N/2$ of the N single-particle energies

$$\varepsilon_j=\pm(4t_0^2\cos^2 k_j+4\alpha^2X^2\sin^2 k_j)^{1/2} \tag{2a}$$

with two electrons up to the Fermi level $\varepsilon_F\le 0$, obtaining the ground-state energy

$$E_0=2\sum_{\varepsilon_j\le\varepsilon_F}\varepsilon_j+NKX^2/2\ . \tag{2b}$$

Evaluating the ground-state energy by minimizing (2b) with respect to X, it turns out that E_0, and even more the degree of dimerization $X_{\min}$ that minimizes E_0, depend *very strongly* on N and on the boundary conditions selected. This is especially true for those small N, for which the full Hamiltonian (1) is numerically tractable (in our case $N\le 10$). With increasing N the dependence on N vanishes, and there is a common limit for all boundary conditions. The convergence is more rapid for larger α.

Applying periodic boundary conditions (PBC's), the allowed wave vectors k_j in Eq. (2a) are $k_j=2\pi j/N$. Thus the Fermi wave vector for the infinite system with half-filled band $k_F=\frac{1}{2}\pi$ is only included for $N=4n$, $n\in\mathbb{N}$. If we use antiperiodic boundary conditions (ABC's), however, $k_F=\frac{1}{2}\pi$ is included for $N=4n+2$. Because the physically most important states are those close to the Fermi surface, we get oscillations in all physical quantities with period four in the number of sites, if we select either periodic or antiperiodic PBC's. In order to avoid these oscillations and increase the number of numerically tractable finite systems with consistent boundary conditions we follow the ideas of Jullien and Martin[20] and introduce a phase angle $\phi\in\mathbb{R}$:

$$c^{\dagger}_{N+1}=c^{\dagger}_1\exp(-i\phi)\ , \tag{3a}$$

$$k_j=2\pi j/N-\phi/N\ . \tag{3b}$$

Periodic boundary conditions (PBC's) correspond to $\phi=0$, antiperiodic boundary conditions (*ABC's*) to $\phi=\pi$. A *monotonous* behavior with N at least for all even N is achieved by choosing $\phi=\phi_0$ for $N=4n$ and $\phi=\phi_0+\pi$ for $N=4n+2$. Taking $\phi_0=0$, we define modified periodic boundary conditions (MPBC's) and modified antiperiodic boundary conditions (MABC's), respectively:

$$\text{MBPC:}\quad \phi=\begin{cases}0, & N=4n\ \ (\text{PBC})\\ \pi, & N=4n+2\ \ (\text{ABC})\ ,\end{cases} \tag{4a}$$

$$\text{MABC:}\quad \phi=\begin{cases}\pi, & N=4n\ \ (\text{ABC})\\ 0, & N=4n+2\ \ (\text{PBC})\ ,\end{cases} \tag{4b}$$

Applying MPBC's, the ground-state energy E_0 ($X=0$) is degenerate in the noninteracting limit, and the system already dimerizes ($X_{\min}\neq 0$) for infinitesimally small α. For MABC's, however, there is a finite-energy difference between the highest occupied and the lowest unoccupied single-particle states [Eq. (2), $\alpha=0$]. Therefore, a finite value of $\alpha>\alpha_c(N)$ is necessary to obtain $X_{\min}\neq 0$, and the small α regime cannot be examined at all on small clusters. It is not possible to treat α and U equivalently with

MABC's. Minimizing Eq. (2b) tells us that there is a *finite* value of dimerization, which is a common limit of both MABC's and MPBC's, in the infinite noninteracting system. Therefore, one cannot expect to obtain correct information about the infinite system by choosing[11] $\alpha(N)=\alpha_c(N)$, which means that there is no dimerization in the noninteracting case. We will show that the modified boundary conditions (4a) and (4b) supply monotonous behavior for all even N and also for $U,V\neq 0$. Previously modified periodic boundary conditions have been used by several studies of the extended Hubbard model,[16–18] whereas former investigations on polymers have mostly preferred PBC's for $4n+2$ systems only,[11–13] which are a special case of MABC, in order to exclude the Jahn-Teller effect, or studied periodic boundary conditions for $4n$ and $4n+2$ systems separately.[14] However, we select MPBC's in our electron-phonon model, as the Peierls distortion observed in the infinite chain operates through a similar mechanism as the Jahn-Teller effect for finite N. A systematic comparison of the influence of different boundary conditions is given for some of our results.

We first calculate all possible electronic configurations for a given value of the total spin projection S_z. According to a theorem by Lieb and Mattis,[21] in one dimension the ground state always belongs to the total spin $S=0$, and can be found in the subspace $S_z=0$, which consists of $\binom{N}{N/2}^2$ configurations. In calculating the matrix representation of the Hamiltonian (1) our algorithm exploits the charge conjugation symmetry for the half-filled band. We use a Lanczos method for real symmetric matrices[22] to calculate eigenvalues and eigenvectors. For the four-site cluster the accuracy of the Lanczos method can be tested by comparing it to exact calculations carried out earlier.[23] The necessary number of Lanczos iterations is chosen in such a way that the analytically known ground-state energy for $U=V=0$ [cf. Eq. (2)] can be reproduced with an accuracy of at least 10^{-12}. According to the limited computer memory available (VAX 8600), we have to restrict ourselves to calculations on 4, 6, 8, and 10 site clusters for the eigenvalue calculations and on 4, 6, and 8 sites, when the calculation of eigenvectors or correlation functions was necessary.

Further on we will use dimensionless values for energies $e_0\equiv E_0/t_0$, $u\equiv U/t_0$, $v\equiv V/t_0$, electron-lattice coupling $\tilde{\alpha}\equiv\alpha(Kt_0)^{-1/2}$ and lattice distortions $x\equiv X(K/t_0)^{1/2}$, which is equivalent to setting $t_0=1$ and $K=1$.

III. PHASES OF THE EXTENDED HUBBARD MODEL

The extended Peierls-Hubbard Hamiltonian (1) combines both electron-lattice ($\tilde{\alpha}$) and electron-electron interactions (u,v). In order to understand the effect of these interactions properly, we use two different approaches: Before we study the full Hamiltonian (1) in Sec. IV C, we will examine the influence of u on dimerization for $v=0$ in Sec. IV A. In this section we discard the coupling to the lattice ($\tilde{\alpha}=0$), and are left with the extended Hubbard model. It should be remarked that this model is, strictly speaking, still an approximation to realistic electron-electron potentials, as the simple Hubbard model has been amended only by a nearest-neighbor term v. Hopping and Coulomb interaction terms beyond nearest neighbors as well as off-diagonal bond-charge repulsion terms are not taken into account. Recently it has been shown, however, that such a treatment is a consistent approximation for a long-range (i.e., weakly screened) electronic potential, relevant, e.g., for undoped polymers that are semiconducting. Most off-diagonal terms and hopping beyond nearest neighbors are of higher order in the overlap matrix element (which is assumed small in any tight-binding approach) of nearest-neighbor wave functions than diagonal terms.[24] Moreover, the extended Hubbard model seems to contain most of the essential physics of longer-ranged potentials.

First we want to examine the transition between charge-density-wave (CDW) and spin-density-wave (SDW) regions, which is found for repulsive interactions $u,v>0$. This transition is known to occur roughly at $u=2v$, but both its exact location and the order of the transition are still disputed in literature.[15–18] From their exact results on a small four-site cluster with periodic boundary conditions Milans del Bosch and Falicov[18] concluded that the transition from CDW to SDW is of first order and occurs exactly on the line $u=2v$. This is in contradiction to previous calculations,[15–17] where a deviation from the Hartree-Fock result $u=2v$ to values u slightly smaller than $2v$ was found. While Hirsch's Monte Carlo results[15] implied a change from a continuous transition to first order for $u\simeq 3$, Fourcade and Spronken concluded both from their renormalization group[16] and finite-cell scaling method[17] that the transition is continuous for all u.

We examine the phase diagram of this model quantitatively by calculating charge and spin correlation functions defined according to Milans del Bosch and Falicov:[18]

$$R_{\mathrm{CNN}}=\langle(N+2\sum_l n_{l\uparrow}n_{l\downarrow}-\sum_l n_l n_{l+1})\rangle/2N\ , \tag{5a}$$

$$R_{\mathrm{CSN}}=\langle(N+2\sum_l n_{l\uparrow}n_{l\downarrow}-\sum_l n_l n_{l+2})\rangle/2N\ , \tag{5b}$$

$$R_{\mathrm{SNN}}=\langle[N-2\sum_l n_{l\uparrow}n_{l\downarrow}+\sum_l\sum_s n_{l,s}(n_{l+1,-s}-n_{l+1,s})]\rangle/2N\ , \tag{5c}$$

$$R_{\mathrm{SSN}}=\langle[N-2\sum_l n_{l\uparrow}n_{l\downarrow}+\sum_l\sum_s n_{l,s}(n_{l+2,-s}-n_{l+2,s})]\rangle/2N\ . \tag{5d}$$

The abbreviations R_{CNN} (R_{SNN}) describes the ground-state expectation values for nearest-neighbor charge (spin) correlations, and R_{CSN} (R_{SSN}) accordingly describes them for second-nearest neighbors. These functions have values between 0 and 1. The charge-density-wave phase is characterized by a large value of R_{CNN} and small R_{SNN}, the spin-density-wave region vice versa. R_{CSN} and R_{SNN} are small in both phases. Although in clusters larger than $N=4$ correlations even higher than second-nearest-neighbor correlations could be observed,

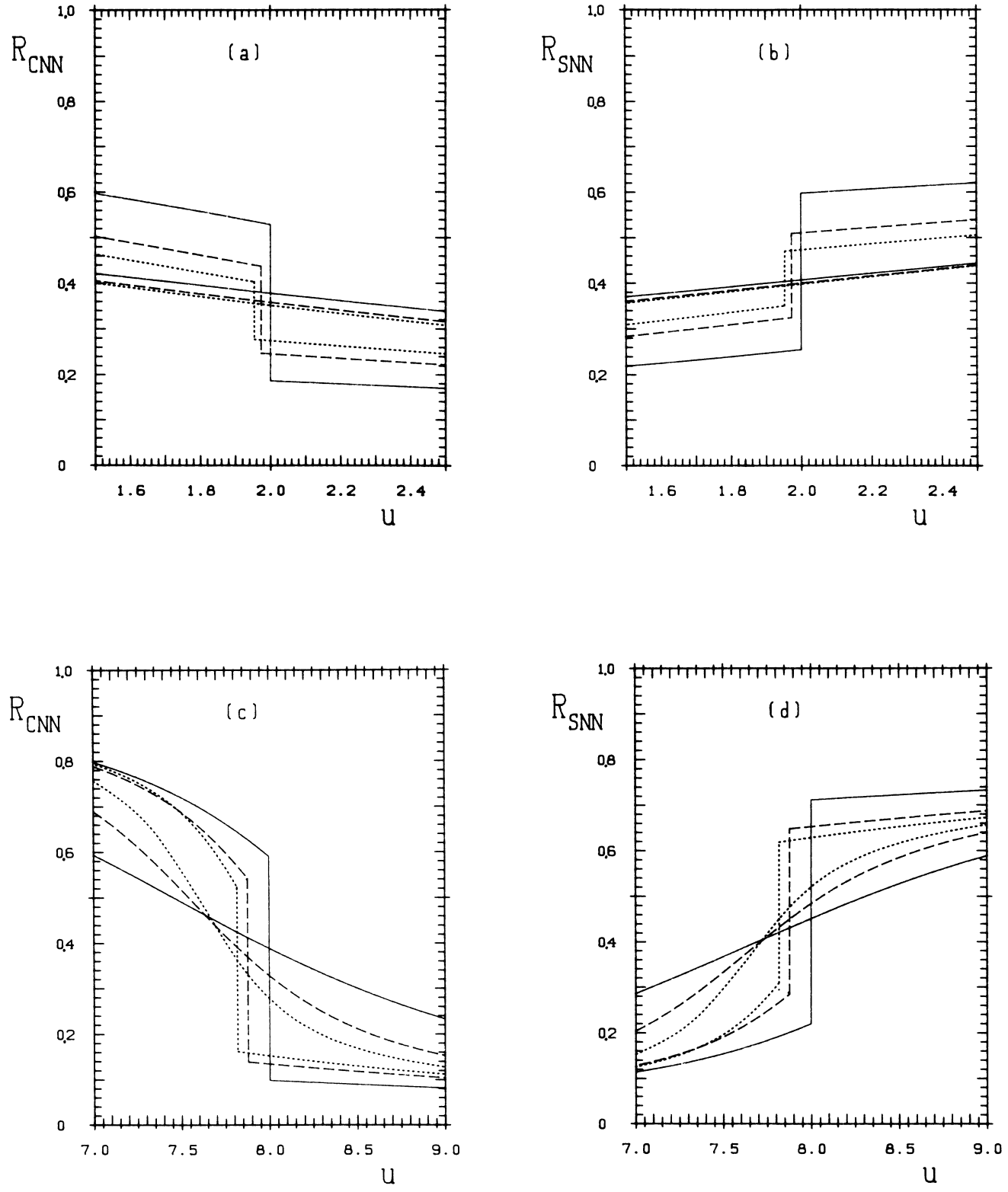

FIG. 1. Ground-state expectation values of the correlation functions R_{CNN} and R_{SNN} as a function of u for $N=4$ (solid), $N=6$ (dashed), and $N=8$ (dotted). The curves with a discontinuity at the corresponding value of Table I are for MPBC's, the continuous curves are for MABC's. (a): R_{SNN} for $N=4$, 6, 8 and $v=1$. (b): R_{SNN} for $N=4$, 6, 8 and $v=1$. (c): R_{CNN} for $N=4$, 6, 8 and $v=4$. (d): R_{SNN} for $N=4$, 6, 8 and $v=4$.

we restrict ourselves to those short-range correlations defined in Eq. (5). In spot checks we also calculated long-range correlation functions defined in a common way as

$$R(2k_F)=\sum_{l=1}^{N}(-1)^l\langle 0(l)0^{\dagger}(1)\rangle \tag{6}$$

with

$$0_{\mathrm{CDW}}=(-1)^l n_l \quad \text{and} \quad 0_{\mathrm{SDW}}=(-1)^l(n_{l\uparrow}-n_{l\downarrow}) .$$

As these ground-state expectation values showed discontinuities at exactly the *same* parameter values $u(v)$, we ensured that the correlation functions defined in Eq. (5) indicate the CDW phase (R_{CNN} large), the SDW phase (R_{SNN} large and $R_{\mathrm{SNN}}\simeq 2R_{\mathrm{SSN}}$) as well as the charge separated (CS) region (R_{CSN} large and $R_{\mathrm{CSN}}\simeq 2R_{\mathrm{CNN}}$) very accurately.

As can be seen from Table I, the CDW-to-SDW transition is found exactly at $u=2v$ only in the special case of a four-site ring ($N=4$). For larger N the transition occurs at a value $u<2v$. The deviation is most significant for medium values of v and slightly increases with the number of sites. According to our limited set of different N, a quantitative extrapolation for the infinite chain is difficult. However, our results indicate a finite departure from the Hartree-Fock result $u=2v$, especially for intermediate v, whereas for very small values $v\to 0$ we find an asymptotic tangential approach to the $u=2v$ line, in agreement with previous results by Fourcade and Spronken (Ref. 16, Fig. 4) as well as analytic calculations[25] based on a continuum representation of the Hamiltonian (1), but in disagreement with others (Ref. 15, Fig. 5 and Ref. 17, Fig. 2), which did not find such an asymptotic approach, shedding some doubts on the reliability of these methods especially for small interactions. For $u,v>>1$ the CDW-SDW interface approaches close to the line $u=2v$ again. Applying MPBC's, we find a finite jump in R_{CNN} and R_{SNN} at the respective transition value $u(v)$ (cf. Table I and Fig. 1), indicating a possible first-order transition. With MPBC's we always find a crossing of two energy levels that belong to states with CDW and SDW structure, respectively, exactly at the transition point, causing a discontinuity in R_{CNN} and R_{SNN}. This discontinuity becomes gradually smaller with decreasing $u\simeq 2v$, but does not vanish for the finite N we can calculate. In Fig. 1 we also show the results for the opposite boundary conditions (MABC's), where we find *no* jump in correlation functions and no crossing of energy levels. When we extrapolate both MPBC and MABC results to a common limit for the infinite system from Fig. 1, however, we find a discontinuous variation in R_{CNN} and R_{SNN}, indicating a first-order transition for large v (e.g., $v=4$) in the infinite system, while there is a continuous transition for small v (e.g., $v=1$). Clearly both MPBC's and MABC's supply a *monotonous* behavior with N, and with increasing N the influence of boundary condition vanishes. When we try to follow the transition line in the direction of increasing interactions, from our calculations for $v=1$, 1.5, and 2, we rather see a gradual than an abrupt change in the order of the transition near $u\simeq 2v\simeq 3$ as Hirsch[15] found it from Monte Carlo calculations. Second-nearest-neighbor correlations R_{CSN} and R_{SSN} are not shown in Fig. 1, as they are small in both regions and insignificant for the CDW-to-SDW transition.

TABLE I. Transition values $u(v)$ from CDW to SDW for $N=4,6,8$ with MPBC's. Correlation functions are discontinuous at these values.

v	$N=4$ (PBC)	$N=6$ (ABC)	$N=8$ (PBC)
0.1	0.200 00	0.199 87	0.199 78
0.2	0.400 00	0.399 19	0.398 56
0.5	1.000 00	0.992 75	0.987 29
1.0	2.000 00	1.972 91	1.953 75
1.5	3.000 00	2.950 54	2.927 79
2.0	4.000 00	3.930 03	3.886 56
4.0	8.000 00	7.877 80	7.817 77
6.0	12.000 00	11.862 1	11.809 9
12.0	24.000 0	23.884 7	23.870 4
20.0	40.000 0	39.920 3	39.918 7

The extended Hubbard model also shows a condensation transition for negative intersite interaction v to a charge separation (CS) region, where all the electrons clump together in one half of the ring.[19] For $N=4$ with PBC, we find that all correlation functions are continuous at this transition, and no condensation transition can be found for repulsive u, even if $v\to-\infty$. Both facts are in disagreement with Ref. 18. However, the four-site model plays a special role, as for $N>4$ the CS ground state is stabilized also for not too large $u>0$. Moreover, for $N>4$ we find an intermediate region (IM) between CS and SDW. In this IM state the edges of the separated charge are softened and built by a singly occupied site (e.g., for $N=8$ this is $\uparrow$, $\uparrow\downarrow$, $\uparrow\downarrow$, $\uparrow\downarrow$, $\downarrow$, 0, 0, 0), instead of the pure CS state (for $N=8$: $\uparrow\downarrow$, $\uparrow\downarrow$, $\uparrow\downarrow$, $\uparrow\downarrow$, 0, 0, 0, 0). For $u>0$ and $v<<-1$ the energy $e(\mathrm{IM})$ of the IM configuration is lower than $e(\mathrm{CS})$ of the CS state, because

$$e(\mathrm{IM})=(N/2-1)4v+(N/2-1)u=e(\mathrm{CS})-u .$$

Therefore for $v<<-1$ the phase boundary from CS to IM is found at $u\to 0+$ in Figs. 3 and 4. The boundary between IM and SDW phases can be calculated from the condition $e(\mathrm{IM})=e(\mathrm{SDW})=Nv$, yielding

$$u=-2v\left[\frac{N-4}{N-2}\right] . \tag{7}$$

This asymptotic behavior is confirmed by our calculations (cf. Figs. 2–4). For smaller $-v$ (>0) hopping becomes important and enlarges the SDW region beyond this line. For $N\to\infty$ the transition to the SDW region approaches the line $u=-2v$, as it was found by Lin and Hirsch.[19] Their Monte Carlo calculations with $N=8,12,\ldots,32$ were insensitive to the difference between CS and IM regions. Surely, as it is a marginal effect, this difference will disappear for $N\to\infty$, but the effect of the boundary is important for finite-size studies and should be considered for correct extrapolations. Using MPBC's, we can clearly identify the transitions from

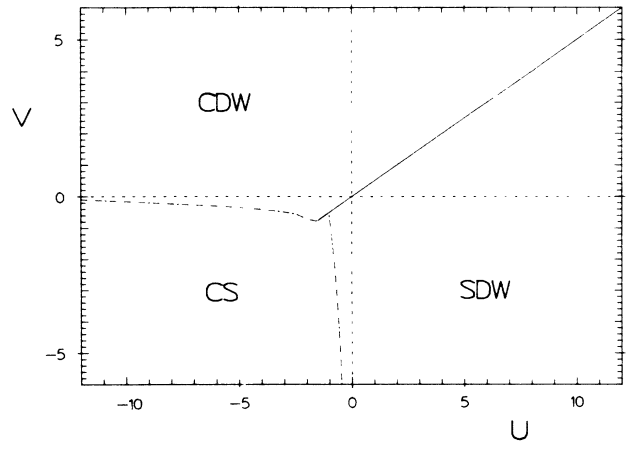

FIG. 2. Phase diagram $u(v)$ for $N=4$ with PBC's. The transition CDW to SDW coincides with the line $u=2v$. At this line R_{CNN} and R_{SNN} are discontinuous, and R_{CSN} and R_{SSN} are continuous. The line $u=2v$ extends into the negative u,v region, but it no longer marks a transition when R_{CSN} is the largest correlation function (in the CS region). Solid lines mark discontinuous transitions; dash-dotted lines mark continuous transitions. Dashed lines indicate the lines $u=0$, $v=0$, and $u=2v$.

CS to IM and from IM to SDW by discontinuous correlation functions for $N>4$. Only for $N=4$, no intermediate region can be observed, because the boundaries between CS and IM, and between IM and SCW, coincide at $u\to 0$. As it was found for the transition from CDW to SDW for repulsive interactions, the discontinuity vanishes if we use MABC's. We find a first-order transition from IM to SDW, which is in good agreement with the transition from CS to SDW found by Lin and Hirsch.[19] The transition from CS to CDW for both $u,v<0$ is found to be continuous for $N=4,6,8$ (compare Figs. 2, 3, and 4). From the phase diagram [$u(v)$ with $u=u/t_0$, $v=V/t_0$ of the extended Hubbard model] for $N=4,6,8$ with MPBC's and the asymptotic behavior for $u,-v\gg 1$ [Eq. (7)] we see that the condensation transition for attractive interactions v shows a larger finite-size dependence than the CDW-to-SDW transition for $v>0$, which is the physically more relevant case.

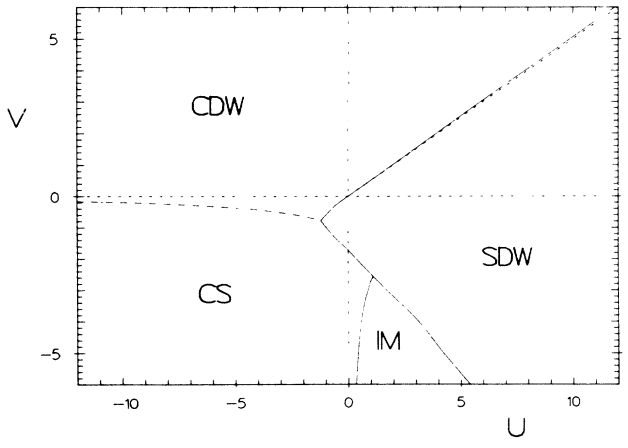

FIG. 3. Phase diagram for $N=6$ with ABC's. The CDW/SDW phase boundary deviates from the line $u=2v$. For $v\ll -1$ the IM region extends from $u=0+$ to $u=-v$. Solid lines mark discontinuous transitions; dash-dotted lines mark continuous transitions. Dashed lines indicate the lines $u=0$, $v=0$, and $u=2v$.

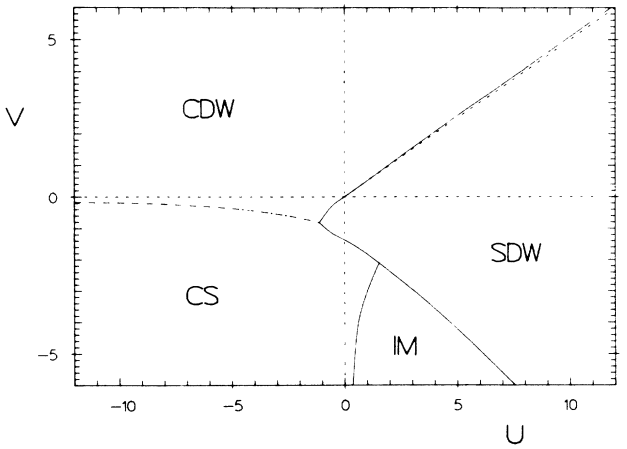

FIG. 4. Phase diagram for $N=8$ with PBC's. The deviations from the line $u=2v$ are slightly larger than in Fig. 3. For $v\ll -1$ the IM region extends from $u=0+$ to $u=-4v/3$. Solid lines mark discontinuous transitions; dash-dotted lines mark continuous transitions. Dashed lines indicate the lines $u=0$, $v=0$, and $u=2v$.

IV. COUPLING TO A STATIC LATTICE AND DIMERIZATION ($x\neq 0$)

A. Influence of the on-site interaction u on dimerization ($v=0$)

Introducing the electron-phonon constant $\tilde{\alpha}$ and the distortion parameter x in our Hamiltonian (1) describes the coupling to a static lattice (SSH-Hubbard model). The alternating sign of $\mp x$ corresponds to alternating single and double bonds changing the transfer element t_0. We always take x as a parameter to minimize the ground-state energy $e_0(x)$ to $e_0(x_{\min})$, obtaining $x_{\min}$ as the degree of dimerization. In order to examine the influence of the Hubbard on-site repulsion u on $x_{\min}$, calculations are carried out for $N=4$, 6, 8, and 10 sites and $v=0$ with modified periodic or antiperiodic boundary conditions. Our results with MPBC's (Figs. 5–7) confirm perturbation theory arguments[12,13] that for small u dimerization depends on the second order of u:

$$x_{\min}(u,N)=a(N)+b(N)u^2 . \tag{8}$$

Using MPBC's Eq. (8) holds very well for $u\leq 1$, whereas it is not true for MABC's (compare Fig. 6). The coefficients $a(N)$ and $b(N)$ *must* have a monotonous size dependence because of our selection of boundary conditions in Sec. II. The $\tilde{\alpha}$ dependence of $a(N)$ is shown in

TABLE II. Dimerization $x_{min}(0,N)=a(N)$ for $u=v=0$ dependence of N for different values of $\tilde{\alpha}$. MPBC results converge from above to the infinite N result, MABC's results from below. For MABC's, dimerization is equal to zero as long as $\tilde{\alpha} \leq \tilde{\alpha}_c(N)$.

N \ $\tilde{\alpha}$	0.4	0.5	0.5659	0.7071	0.8	1
4 (PBC)	0.4	0.5	0.5659	0.7071	0.8	1
6 (ABC)	0.2841	0.3686	0.4297	0.5800	0.6967	1
8 (PBC)	0.2254	0.3030	0.3635	0.5286	0.6660	1
10 (ABC)	0.1893	0.2629	0.3244	0.5048	0.6567	1
∞	0.0272	0.1283	0.2294	0.4831	0.6528	1
10 (PBC)	0	0	0	0.4532	0.6486	1
8 (ABC)	0	0	0	0.3996	0.6366	1
6 (PBC)	0	0	0	0	0.5766	1
4 (ABC)	0	0	0	0	0	1

Table II: $a(N)=x_{min}(0,N)$ can be obtained analytically from exact one-particle calculations for arbitrary N [Eq. (2)], confirming our diagonalization results exactly for $N \leq 0$. $a(N)$ converges towards a nonzero limit $a(\infty)$ as $N \rightarrow \infty$, namely, from above for MPBC's and from below for MABC's (cf. Table II). For small α this limit can be obtained[13] analytically as

$$\alpha(\infty)=(4/\tilde{\alpha})\exp[-1-\pi/(4\tilde{\alpha}^2)].$$

Minimizing Eq. (2) for very large N (e.g., $N=10\,000$), we find approximately a linear dependence of $a(\infty)$ on $\tilde{\alpha}$ in the large $\tilde{\alpha}$ region, where this expression no longer holds (cf. Table II). Using MABC's, however, dimeriza-

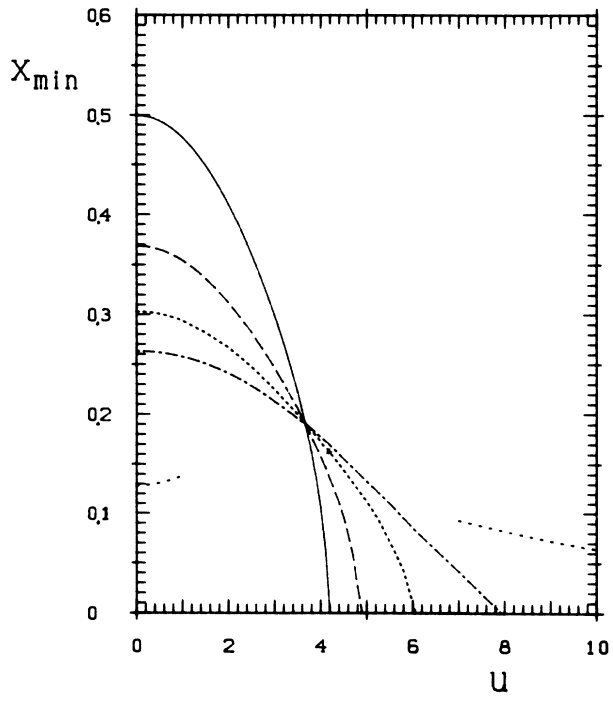

FIG. 5. Dimerization $x_{min}(u)$ for $\tilde{\alpha}=0.5$, $v=0$ and MPBC's: $N=4$ (solid), $N=6$ (dashed), $N=8$ (dotted), and $N=10$ (dash dotted). There is an N-independent point at $u_0=3.66$. The unfinished dotted line increasing with u^2 for small $u \leq 1$ indicates our extrapolated result for $N \rightarrow \infty$. The dotted line for large u marks a result of spin-Peierls theory (Ref. 27) for $N \rightarrow \infty$.

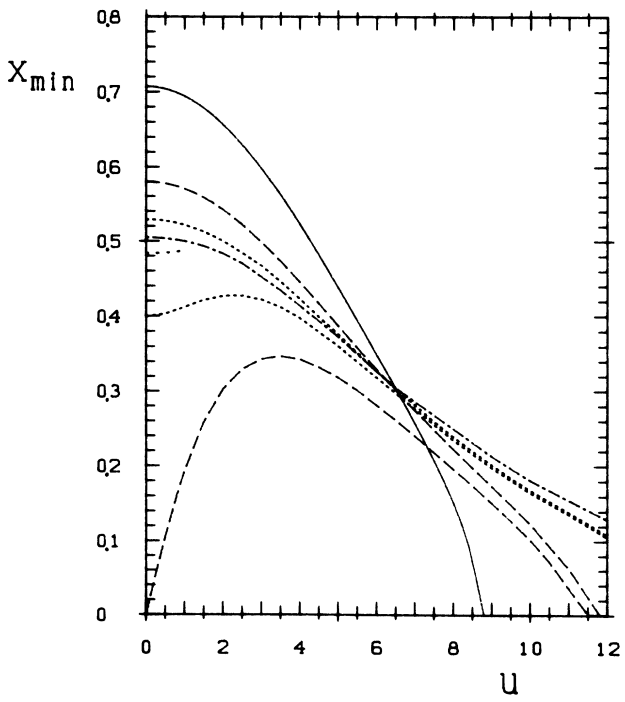

FIG. 6. Dimerization $x_{min}(u)$ for $\tilde{\alpha}=(0.5)^{1/2}=0.7071$, $v=0$ and $N=4$ (solid), $N=6$ (dashed), $N=8$ (dotted), and $N=10$ (dash dotted). For $N=6$ and 8 we show both MPBC's results, which decrease for small u with u^2, and MABC results, which increase for small u but remain lower than the MPBC results. For MPBC's, there is an N-independent point at $u_0=6.51$. Already for $N=8$, the influence of boundary condition vanishes for large u. The unfinished dotted line increasing slowly with u^2 for small $u \leq 1$ indicates our extrapolated result for $N \rightarrow \infty$.

tion is exactly equal to zero as long as $\tilde{\alpha} \leq \tilde{\alpha}_c(N)$. Because of the finite difference in energy between the highest occupied and the lowest occupied levels, a finite minimum value of electron-lattice coupling $\tilde{\alpha}_c(N)$ is necessary for $N < \infty$ with MABC's. This critical value of $\tilde{\alpha}_c(N)$ is quite large for those N which can be treated in numerical calculations, e.g., $\tilde{\alpha}_c(4) = 2^{1/4} \simeq 0.8409$ and $\tilde{\alpha}_c(6) = 2^{-1/2} \simeq 0.7071$. On the other hand, when we use MPBC's, the Fermi level corresponds to an allowed wave vector and is half occupied. Because of the degeneracy of the ground state we find a nonzero dimerization already for an infinitesimally small coupling $\tilde{\alpha}$. Therefore, MPBC's must be used in order to obtain information relevant for systems with small $\tilde{\alpha}$. Our calculations with $\tilde{\alpha} = 0.5$ (shown in Fig. 5) could not be performed with MABC's, because $\tilde{\alpha} = 0.5 < \tilde{\alpha}_c(N)$ for $N \leq 26$. The results shown in Fig. 6 correspond to $\tilde{\alpha} = 2^{-1/2} \simeq 0.7071 = \tilde{\alpha}_c(6)$. In this case we can also use MABC's for $N = 6$ (PBC) and $N = 8$ (ABC). Obviously the dimerization obtained with MABC's is always smaller than with MPBC's for the same number of sites N (cf. Fig. 6), buy for large u the influence of different boundary conditions vanishes.

There is a maximum physical value of $\tilde{\alpha}$; it is obtained by the condition $\tilde{\alpha}_D x_{\min} = 1$ (or $t_0 = \alpha_D X_{\min}$), the case of *fully decoupled dimers* with $t_l = 0$ and $t_{l+1} = 2t_0$. In the noninteracting case, we find $\tilde{\alpha}_D = 1$, $x_{\min} = 1$, and the ground-state energy per site $e_0(x_{\min})/N = -\frac{3}{2}$ independent of the number of sites for both MPBC's and MABC's with $N \geq 4$. In the limit $\tilde{\alpha}_D = 1$ the dimerization for $u = 0$ is $a(N) = 1$ independent of N, whereas the decrease with u is slightly N dependent. We can treat the case of *decoupled dimers* by assuming that every second transfer term is equal to zero also for $u \neq 0$. Then the ground-state energy is

$$(2/N)e_0 = u/2 + x^2 - [u^2/4 + 4(1+\tilde{\alpha}x)^2]^{1/2}. \tag{9}$$

The equation to determine $x_{\min}$ reads

$$16(x^2 - \tilde{\alpha}^2)(1+\tilde{\alpha}x)^2 + u^2 = 0 . \tag{10}$$

Assuming $x_{\min} = 1 + b\,u^2$, we obtain necessarily $\tilde{\alpha} = 1$ and

$$b = -1/128 . \tag{11}$$

We notice that the assumption of decoupled dimers using $\tilde{\alpha} = 1$ for $u > 0$ must be an approximation: As $x_{\min}$ decreases with U also for $\tilde{\alpha} = 1$, one would have to use $\tilde{\alpha}_D > 1$ in order to get really *decoupled dimers* for $u > 0$. Nevertheless, the preceding (variational) result provides an estimate of $b(\infty)$ for $\tilde{\alpha} = 1$. The most important conclusion is that the *sign* of $b(\infty)$ is *negative* for $\tilde{\alpha} = 1$.

The coefficient $b(N)$ was evaluated by fitting our results with MPBC's to Eq. (8), which proved to be very well satisfied for $u \leq 1$. Improving earlier calculations,[26] we determined $b(N)$ with an accuracy of 3×10^{-4} for $N = 10$ and 2×10^{-5} for $N = 4$, 6, 8 and different values of $\tilde{\alpha}$. The results are shown in Fig. 7 as a function of $\tilde{\alpha}$. We found that $b(N)$ is approximately proportional to $1/N$, but there are considerable deviations from this proportionality, which become more obvious for large $\tilde{\alpha}$. Therefore we performed least-squares fits of our results to the curves

$$b(N) = b_0 + b_1/N + b_2 g(N) \tag{12}$$

using various functions $g(N) = 1/N^2, 1/N^3, 1/N^4, 1/(N \ln N), 1/(N^2 \ln N)$. The results for $b_0 = b(\infty)$ using different functions $g(N)$ deviate by less than 3×10^{-3} from the best value marked in Fig. 7 by circles. The dotted line in Fig. 7 is the result obtained by expanding the formula of Baeriswyl and Maki [Ref. 13, Eq. (20)] to the order u^2. In this evaluation $b_0(\tilde{\alpha})$ reaches a maximum near $\tilde{\alpha} \simeq 0.5$, but the equation is only exact for small $\tilde{\alpha} \ll 1$. Figure 7 shows that the agreement is quite good for $\tilde{\alpha} < 0.5$. For medium values of the electron-phonon coupling ($\tilde{\alpha} \simeq 0.5$), which are relevant for $(CH)_x$, our extrapolated result for b_0 is smaller than the analytic expansion of Baeriswyl and Maki. Clearly, for small $\tilde{\alpha}$ we also find that b_0 becomes *positive*. As we have seen that b_0 is *negative* for $\tilde{\alpha} = 1$, and the dependence of b_0 on $\tilde{\alpha}$ is continuous, there must be a critical value of $\tilde{\alpha}_0$, for which a crossover from dimerization enhancement to suppression of dimerization with u occurs in the infinite system. Our extrapolated values $b_0(\tilde{\alpha})$ in Fig. 7 yield $b_0(\tilde{\alpha}_0) = 0$ for $\tilde{\alpha}_0 = 0.75(\pm 0.04)$. This value corresponds surprisingly well with the one found by Baeriswyl and Maki by a

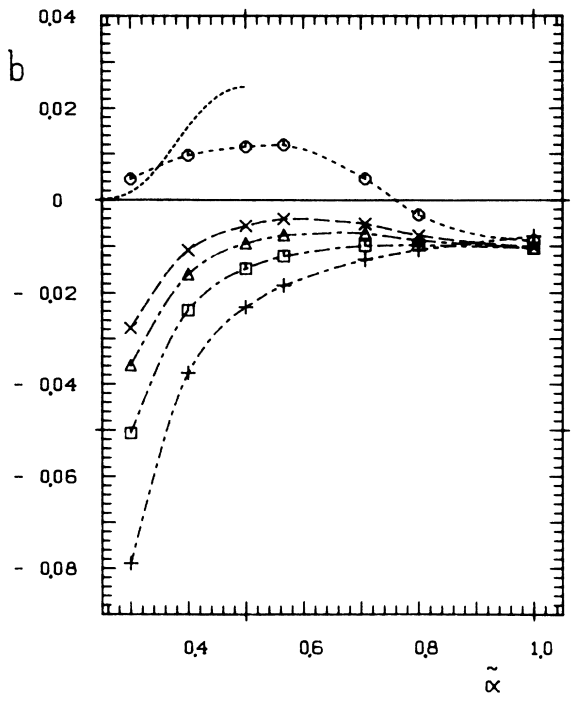

FIG. 7. The coefficient b of Eq. (8) in dependence of $\tilde{\alpha}$ for $N = 4$ (+), $N = 6$ (squares), $N = 8$ (triangles), and $N = 10$ (×). Our extrapolated results for $N = \infty$ are indicated by circles. The dotted curve marks the evaluation of the result of Baeriswyl and Maki [Ref. 13, Eq. (20)], valid for small $\tilde{\alpha}$. For any given parameters α, K and $U \leq t_0$ dimerization is given by $X_{\min} = a(t_0/K)^{1/2} + b(t_0 K)^{-1/2} U^2$, and $\tilde{\alpha} = \alpha(K t_0)^{-1/2}$.

different approach: $\lambda_0=2\tilde{\alpha}_0^2/\pi=0.37$ or $\tilde{\alpha}_0=0.76$.

For small $\tilde{\alpha}$ there is further support for an enhancement of dimerization by u in the infinite system: We always find a finite value u_0, for which the degree of dimerization $x_{\min}(u_0,N)$ is independent of N (cf. Figs. 5 and 6), if we use MPBC's. As the boundary conditions were chosen in a way that provides *monotonous* behavior with N (cf. Sec. II), those N-independent points *must* also be points of the dimerization curve of the infinite chain. Thus, for any fixed value of $\tilde{\alpha}$, we get *two* points ($u=0$ and $u=u_0$) of the curve for the infinite system. For small $\tilde{\alpha}$ we find $x_{\min}(0,\infty)<x_{\min}(u_0,N)$. Therefore the dimerization $x_{\min}(u,\infty)$ has to increase with u first to pass through the N-independent point $x_{\min}(u_0,N)$.

In order to get an idea of the behavior of the infinite chain for large values of u, one can use a result of the spin-Peierls theory with the self-consistent harmonic approximation (SCHA) by Kuboki and Fukuyama [Ref. 27, Eq. (5.13)]. This result is also shown in Fig. 5 (dotted line):

$$x_{\min}(u,\infty)=9.34\tilde{\alpha}^2(1/u-9.16/u^3)^{3/2}\ . \tag{13}$$

As the expansions were taken until fourth order in $1/u$, the resulting curve can be evaluated only for $u\gg 1$.

B. Application to polyacetylene

There is a considerable uncertainty in the value of $\tilde{\alpha}=\alpha(Kt_0)^{-1/2}$ appropriate for trans-$(CH)_x$, since especially α and K are not precisely known from experiments: The parameters most frequently used for polyacetylene[4,8] were obtained by Su, Schreiffer, and Heeger for the noninteracting case. They correspond to an intermediate coupling $\tilde{\alpha}_{\rm SSH}=0.5659$, which still implies a dimerization enhancement. However, there are quite different estimations for the electron-lattice coupling—[$\alpha=3.7$ eV Å^{-1} (Ref. 10), $\alpha=3.9$ eV Å^{-1} (Ref. 13), $\alpha=4.1$ eV Å^{-1} (Refs. 4 and 14) and $\alpha=4.5$–6.0 eV Å^{-1} (Ref. 12)] and the force constant [$K=21$ eV Å^{-2} (Refs. 4 and 14), $K=31$ eV Å^{-2} (Ref. 12), and $K=35$ eV Å^{-2} (Refs. 10 and 13)], whereas the best known property is the bandwidth $4t_0=10$ eV (Refs. 4, 12, and 14), but even for t_0 different values have been used [$t_0=1.6$ eV (Ref. 10) and $t_0=2.9$ eV (Ref. 13), respectively]. In our units ($K=t_0=1$) these estimations result in $\tilde{\alpha}_{\rm SSH}=0.57$ (Refs. 4, 8, and 14), $\tilde{\alpha}=0.49$ (Ref. 10), $\tilde{\alpha}=0.39$ (Ref. 13), or $\tilde{\alpha}=0.51$–0.68 (Ref. 12).

More recent experimental data[28] indicate $K=\frac{3}{4}*46$ eV Å^{-2} and $4t_0=(12.8\pm0.5)$ eV. Using the value $\alpha=4.1$ eV Å^{-1} obtained by SSH in the noninteracting picture, this would imply rather a smaller value for the reduced coupling constant $\tilde{\alpha}=\alpha(Kt_0)^{-1/2}=0.39$. So it seems that in polyacetylene dimerization must be enhanced by u, as $\tilde{\alpha}<0.75$, but even a large $\tilde{\alpha}$ behavior ($\tilde{\alpha}>0.75$) cannot fully be excluded. Finally, we see that the location of the dimerization maximum depends very strongly on $\tilde{\alpha}$, and cannot generally be found near $u\simeq 4t_0$, as it was proposed earlier.[11,13]

C. Influence of the intersite interaction v

In Sec. IV A we have examined the influence of an on-site interaction u on dimerization without an interaction between neighboring sites ($v=0$), whereas in Sec. III we have studied the extended Hubbard model without coupling to a lattice ($\tilde{\alpha}=0$). However, both electron-phonon and extended electron-electron interactions are important in order to describe experimental results correctly. Although some experiments can be fitted reasonably well with $v=0$, the estimated value for u may change by a factor of 2, if also a nearest-neighbor interaction $v\simeq u/2$ is taken into account.[6] There are also theoretical reasons for the importance of electron-electron interactions beyond the simple Hubbard model: These must be taken into account for weakly screened potentials, as they are expected in a semiconductor like polyacetylene. Therefore we will now study the influence of finite v.

When we calculate ground-state correlation functions for finite N with MPBC's as a function of u and v, we find no discontinuities in the dimerized system (with $x_{\min}\neq 0$) as we did in Sec. III with MPBC's, but a smooth transition region, where charge and spin correlations are smaller than in the undimerized system. There is no longer a crossing of energy levels, since these are already split by the Peierls instability for $x\neq 0$. We examined the influence of v on dimerization by calculating $x_{\min}(u,v)$ for fixed values of v for $N=4,6,8$ with MPBC's. The results for $v=4$ are shown in Fig. 8 for two different values of $\tilde{\alpha}$: In our calculations on finite systems, the maximum dimerization is always found at $u\simeq 2v$, independent of $\tilde{\alpha}$, more precisely at $u=2v$ exactly for $N=4$ and at a value slightly below $u=2v$ for $N>4$. We find that the region of u with nonzero dimerization becomes smaller with increasing v and with decreasing $\tilde{\alpha}$. Figure 8 also shows that dimerization is suppressed rapidly for $u<2v$ ("CDW region"), even more rapidly with increasing N, whereas for $u>2v$ ("SDW region") the region with $x_{\min}\neq 0$ enlarges with N and spreads until $u\to\infty$ for infinite N.

We notice a connection to the pure extended Hubbard model on a rigid lattice: In our finite-size calculations maximum dimerization is always found at the *same* value of $u(v)$, where the phase separation between SDW and CDW was found in Sec. III (cf. Table I). This transition is connected with a crossing of the lowest-energy levels. Perturbation theory shows that the energy gain by dimerization and with it $x_{\min}$ itself is largest exactly at the intersection of the two lowest-energy levels. We believe that the dimerization maximum occurring close to but not exactly at $u=2v$ is a noteworthy result for several reasons.

(1) There is no general reason for this to be the case in interacting electron-phonon systems; e.g., it was demonstrated earlier[29] in the framework of a continuum theory that significant deviations do occur if one allows for phonon quantum fluctuations. That theory predicts a dimerization maximum $u=2v$ only for the phonon frequency tending towards zero, as in the case in our study. In the limit $u\simeq 2v\to 0$ where Ref. 29 applies, we reproduce this behavior through our connection to the extended Hubbard model.

(2) Deviations from $u=2v$ do occur at intermediate coupling, which we believe to persist in the $N\rightarrow\infty$ limit. At intermediate coupling, the dimerization maximum in our study occurs for $u<2v$. Notice that the critical u scales to smaller values with increasing N. Assuming monotonous finite-size scaling then implies a finite deviation from $u=2v$ for $N\rightarrow\infty$. Moreover, Monte Carlo results on the extended Hubbard model with up to 32 sites[15] find a finite deviation for the CDW/SDW interface from $u=2v$ (in agreement with our Sec. III) and imply the same deviations through our level crossing argument.

V. CONCLUSIONS

In Sec. III we determined the phase diagram $u(v)$ of the extended Hubbard model with half-filled band. By finite-size analysis of exact diagonalization results on small clusters with consistent boundary conditions (Sec. IV A), we have seen that in the thermodynamic limit dimerization is enhanced by small u for $\tilde{\alpha}<0.75$ (±0.04) and decreases with u for large $\tilde{\alpha}$. Additionally to this extrapolated behavior for small u we always find a fixed (N independent) point $x_{\min}(u_0,\infty)$, using modified periodic boundary conditions. Comparing our results quantitatively with previous ones, we find good agreement with Hirsch[8] and Hayden and Soos,[14] and it seems that dimerization enhancement has been slightly overestimated by Baeriswyl and Maki.[13] We have to notice a possible mixing up of the value for the coupling constant $\lambda=2\tilde{\alpha}^2/\pi$ defined by Baeriswyl and Maki[13] with the usual electron-phonon coupling α of the SSH-Hubbard model: Hirsch's Monte Carlo data[8] correspond to $\alpha=0.29$, $K=0.25$, $t_0=1$, which means $\tilde{\alpha}=0.58$ and $\lambda=0.21$, but not to $\lambda=0.29$, as stated by Baeriswyl and Maki (Ref. 13, Fig. 1) and by Hayden and Soos (Ref. 14, Fig. 8). The reproduction of Hirsch's data in both figures must be reduced by a factor of 2 (cf. Ref. 8, Fig. 1) to obtain the correct value $\delta_0=\tilde{\alpha}x_{\min}$. The data now agree very well with the results by Hayden and Soos (Ref. 14, Fig. 8) for $\lambda=0.20$ and with our results for $\tilde{\alpha}=0.5659$ ($\lambda=0.2038$).

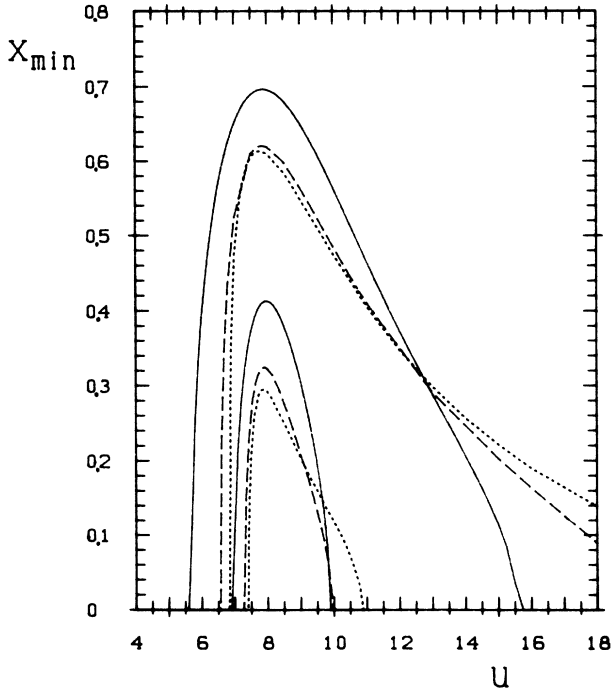

FIG. 8. Dimerization $x_{\min}(u)$ for $v=4$ with MPBC's for $N=4$ (solid), $N=6$ (dashed), and $N=8$ (dotted) for two different electron-lattice couplings $\tilde{\alpha}$: The upper curves correspond to $\tilde{\alpha}=0.8$, the lower ones to $\tilde{\alpha}=0.5$. The maximum of dimerization is found at $u=2v=8$ for $N=4$, and slightly below this value for $N=6,8$, independent of $\tilde{\alpha}$.

In the last Sec. IV C we have shown that a nearest-neighbor repulsion v shifts the maximum of dimerization from $u=0$ to a value $u\leq 2v$, which is in fact the same value, where the transition from a CDW to a SDW ground state was found in the extended Hubbard model ($\tilde{\alpha}=0$).

Finally, we note that we have demonstrated the importance of finite-size effects in exact numerical calculations on small systems. In fact, we have shown explicitly (cf., e.g., Fig. 7) that the response of some physical quantity characterizing the system to a change in one of its parameters (in our case dimerization and u, respectively) may be *opposite* in small and large systems. Many contradictory results on the influence of electronic interactions on the dimerization amplitude in the SSH model can be traced to both finite-size effects and the treatment of boundary conditions. In one dimension (1D) we have demonstrated that modified boundary conditions are a useful tool guaranteeing monotonous variation with system size, which is primordial for any systematic finite-size analysis. The problem of consistent boundary conditions is still to be solved in 2D, where finite-size effects are expected to be at least as important as in 1D (if the total number of sites of the system is the relevant quantity) or even more (if the lateral extension of a lattice is decisive). Available studies on small two-dimensional systems do not yet address these issues, and it will be interesting to see if their conclusions are modified once such more systematic investigations are performed.

During the revision of our manuscript, a paper by Kuprievich[30] was published, obtaining results comparable to Sec. IV A by *approximate* calculations (deviations from exact energies are about 20% for $N=6$ and $N=10$; cf. Ref. 30, Table I) with $N=50$ and PBC. This author finds the critical value of $\tilde{\alpha}_0$ "a bit smaller than 0.75," which is in good agreement with our result. However, no extrapolation to the infinite limit was performed, although for small $\tilde{\alpha}\leq 0.5$ the finite-size effect is still obvious [Ref. 30, Fig. 2]: For small u Kuprievich's results (with $N=50$ and MABC's) deviate from the prediction of Baeriswyl and Maki's $x_{\min}=a+bu^2$, which was confirmed by our calculations (with MPBC's) for both small and large $\tilde{\alpha}$.

ACKNOWLEDGMENTS

We acknowledge very useful discussions with A. Painelli. One of us (J.V.) would like to thank E. Y. Loh, Jr. for helpful correspondence and G. W. Hayden for sending us Ref. 14 prior to publication.

*Also at Bayreuther Institut für Makromolekülforschung.
[1]J. Hubbard, Proc. R. Soc. London, Ser. A **276**, 238 (1963); **277**, 237 (1964); **281**, 401 (1964); **285**, 542 (1965); **296**, 82 (1966); **296**, 100 (1967).
[2]Proceedings of the International Conference on High-Temperature Superconductors, Interlaken, 1988 [Physica C **153-155** (1988)]; F. C. Zhang, and P. Prelovsek, Phys. Rev. B **37**, 1569 (1988).
[3]For reviews of recent progress, see Proceedings of the International Conference on Synthetic Metals, Sante Fe, 1988 [Synth. Met. **27** (1988); **27-29** (1989)].
[4]W. P. Su, J. R. Schrieffer, and A. J. Heeger, Phys. Rev. Lett. **42**, 1698 (1979); Phys. Rev. B **22**, 2099 (1980).
[5]H. Thomann, L. R. Dalton, Y. Tomkiewicz, N. S. Shiren, and T. C. Clarke, Phys. Rev. Lett. **50**, 533 (1983).
[6]A. Grupp, P. Höfer, H. Käss, M. Mehring, R. Weizenhöfer, and G. Wegner, in *Electronic Properties of Conjugated Polymers,* edited by H. Kuzmany, M. Mehring and S. Roth (Springer, Berlin, 1987).
[7]B. R. Weinberger, C. B. Roxlo, S. Etemad, G. L. Baker, and J. Orenstein, Phys. Rev. Lett. **53**, 86 (1984).
[8]J. E. Hirsch, Phys. Rev. Lett. **51**, 296 (1983).
[9]L. G. Caron and C. Bourbonnais, Phys. Rev. B **29**, 4230 (1984); V. Ya. Krinov and A. A. Ovchinnikov, Zh. Eksp. Teor. Fiz. **90**, 709 (1986).
[10]P. Horsch, Phys. Rev. B **24**, 7351 (1981).
[11]S. N. Dixit and S. Mazumdar, Phys. Rev. B **29**, 1824 (1984); S. Mazmudar and S. N. Dixit, Phys. Rev. Lett. **51**, 292 (1983).
[12]S. Kivelson and D. E. Heim, Phys. Rev. B **26**, 4278 (1982).
[13]D. Baeriswyl and K. Maki, Phys. Rev. B **31**, 6633 (1985).
[14]G. W. Hayden and Z. G. Soos, Phys. Rev. B **38**, 6075 (1988).
[15]J. E. Hirsch, Phys. Rev. Lett. **53**, 2327 (1984).
[16]B. Fourcade and G. Spronken, Phys. Rev. B **29**, 5089 (1984).
[17]B. Fourcade and G. Spronken, Phys. Rev. B **29**, 5096 (1984).
[18]L. Milans del Bosch and L. M. Falicov, Phys. Rev. B **37**, 6073 (1988).
[19]H. Q. Lin and J. E. Hirsch, Phys. Rev. B **33**, 8155 (1986).
[20]R. Jullien and R. M. Martin, Phys. Rev. B **26**, 6173 (1982).
[21]E. H. Lieb and D. Mattis, Phys. Rev. **125**, 164 (1962).
[22]J. K. Cullum and R. A. Willoughby, *Lanczos Algorithms for Large Symmetric Eigenvalue Computations* (Birkhäuser, Boston, 1985).
[23]J. Takimoto and Y. Toyozawa, J. Phys. Soc. Jpn. **52**, 4331 (1983).
[24]A. Painelli and A. Girlando, Synth. Met. **27**, A15 (1988).
[25]J. Voit (unpublished).
[26]V. Waas, J. Voit, and H. Büttner, Synth. Met. **27**, A21 (1988).
[27]K. Kuboki and H. Fukuyama, J. Phys. Soc. Jpn. **56**, 3126 (1987).
[28]E. Ehrenfreund, Z. Vardeny, O. Brafman, and B. Horovitz, Phys. Rev. B **36**, 1535 (1987); J. Fink and G. Leising, Phys. Rev. B **34**, 5320 (1986).
[29]J. Voit, Phys. Rev. Lett. **62**, 1053 (1989); and in Interacting Electrons in Reduced Dimensions, Proceedings of NATO Advanced Research Workshop, Torino (Plenum, New York, in press).
[30]V. A. Kuprievich, Phys. Rev. B **40**, 3882 (1989).